Comparison of optical detection system, PVDF detection system, and PVDF needle hydrophone for optoacoustic tomography

M. D. Abolhassani[1], M. Hejazi[1], A. Ahmadian[1], and A. Amjadi[2]

[1] *Medical Physics and Bioengineering Department, Faculty of Medicine, Tehran University of Medical Sciences, Tehran, Iran; & Research Centre for Science and Technology in Medicine, RCSTIM*

[2] *Institute of Physics, Sharif University, Tehran, Iran*

Received January 10, 2005

Optoacoustic tomography (PAT) is a two-dimensional medical imaging method that has the advantage of optical contrast and resolution of ultrasonic waves. The detection systems with a high sensitivity can be used for detecting small tumors, located deeply in human tissues, such as the breast. In this study, the sensitivity of existing ultrasonic detection systems has been compared experimentally with that by using thermoelastic waves as a broadband ultrasonic source. For the comparison, an optical stress transducer (OST), a polyvinylidene difluoride (PVDF) sheet and a calibrated PVDF needle hydrophone were used. To ensure all of the detection systems interrogated by the same ultrasonic field, a small optical instrument that fixed the generating laser head was constructed. The sensitivity was evaluated by measuring signal-to-noise ratios (SNRs) and noise equivalent pressures (NEPs). The PVDF system, with a 4-kPa NEP has a 22 dB better performance than the OST. The OST showed nearly the same sensitivity as the hydrophone for detecting ultrasound waves at a 1-cm distance in water. PVDF detection system provides a useful tool for imaging of soft tissues because of its high sensitivity and broad detection range.

OCIS codes: 120.3890, 170.5120.

Optoacoustic tomography (PAT) is a two-dimensional (2D) medical imaging method that has the advantage of optical contrast and resolution of ultrasonic waves. This modality has many applications in biomedical imaging fields such as detection of layered structures of tissues or tumors under human epidermis[1], deeply embedded tumors, e.g. breast tumors[2], and photoacoustic tomography for obtaining the images of mouse brain[3]. In PAT, tissue chromophores rapidly expand after irradiation with nanosecond laser pulses. The thermoelastic expansion of the absorbers creates acoustic waves. The waves propagate toward the surface of the tissues where they are detected by ultrasound detectors. There are two types of ultrasonic transducers used in PAT, optical and piezoelectric.

Beard *et al.* compared acoustic performance of a low finesse Fabry-Perot (FP) interferometer with that of a polyvinylidene difluoride (PVDF) needle and membrane hydrophones. A peak noise-equivalent-pressure (NEP) of FP was 10 kPa over a 25-MHz measurement bandwidth[4]. A new FP in conjunction with a balanced photodetector has been developed which provided a NEP of 0.35 kPa over a 20-MHz measurement bandwidth. The sensitivity achieved with this type of sensors is comparable to that of a 1-mm diameter PVDF element[5]. Oraevsky *et al.* used a 0.5-mm-thick PVDF slab with the sensitivity of 1.5 V/bar[6]. The sensitivity of optical stress transducer (OST) was obtained 1.68 bar^{-1} by Köstli *et al.*[7]. Hamilton *et al.* calculated the sensitivity of an ideal piezoelectric element as 2.2×10^{-8} $\mathrm{nm}/\sqrt{\mathrm{Hz}}$ at 50 MHz[8].

The goal of this paper is to develop an experimental setup with pulsed laser and absorbing liquid for measuring sensitivity and bandwidth of detection systems under the same experimental conditions. The sensitivity of three types of detection systems, OST, PVDF, and needle hydrophone was measured by measuring their signal-to-noise ratios (SNRs) and NEPs.

The OST consists of two prisms, which are attached to a thick infrasil glass plate. The sensor surface is illuminated with a continuous probe laser and immersed in water (Fig. 1). Acoustic waves are incident on the glass plate, modulating the glass and water refractive indices, thereby changing the optical reflectance of the probe beam at the glass-water interface. The optical reflectance R_0 can be derived from the Fresnel formula

$$R_0 = 0.5 \left[\left(\frac{\sin(\gamma_\mathrm{w} - \gamma_\mathrm{g})}{\sin(\gamma_\mathrm{w} + \gamma_\mathrm{g})} \right)^2 + \left(\frac{\tan(\gamma_\mathrm{w} - \gamma_\mathrm{g})}{\tan(\gamma_\mathrm{w} + \gamma_\mathrm{g})} \right)^2 \right], \quad (1)$$

where γ_g is the angle of incidence at glass-water interface and γ_w is the angle of refraction in water. The angles are related according to Snell's law

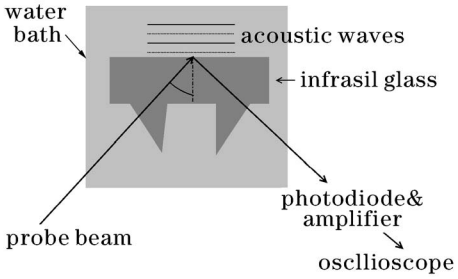

Fig. 1. Scheme of the OST. The photodiode measures pressure-induced changes of the refraction index at the glass-water interface.

$$n_{\rm g} \sin\gamma_{\rm g} = n_{\rm w} \sin\gamma_{\rm w}, \tag{2}$$

where $n_{\rm g}$ and $n_{\rm w}$ are the refractive indices of glass and water, respectively. The relation of refractive index n at pressure p and refractive index n_0 at ambient pressure is given by

$$n = n_0 + \frac{{\rm d}n}{{\rm d}p} p. \tag{3}$$

Hence the sensitivity S of the optical transducer can be defined as

$$S = \frac{1}{R_0} \frac{{\rm d}R}{{\rm d}p}, \tag{4}$$

where R_0 is the reflectance at ambient pressure[9,10].

As probe beam, a frequency doubled Nd:YAG laser (λ = 532 nm) was used. The probe beam illuminated an elliptical spot on the glass-water interface, with principal diameters of about 200 and 250 μm. The reflected light from the spot, with the reflectance of 0.83 at ambient pressure, was recorded by a photodiode (DT-25). The theoretical sensitivity was calculated by ${\rm d}n_{\rm g}/{\rm d}p = 1.08\times10^{-6}$ bar^{-1}, ${\rm d}n_{\rm w}/{\rm d}p = 1.35\times10^{-5}$ bar^{-1} (taken from Ref. [10]), $n_{\rm g}$ = 1.460 and $n_{\rm w}$ = 1.333 at λ = 532 nm. The sensitivity S and the reflectance at the ambient pressure, as functions of the incident angle, are shown in Fig. 2. The sensitivity of the detector increases as the incident angle of the probe beam approaches the critical angle for total internal reflection. Hence, the theoretical sensitivity was derived to be about 0.0083 bar^{-1}, with R_0 = 0.83 and the angle of incidence close to 66°.

As a compressive wave is incident on the glass-water interface, the difference between the refractive indices of water and glass decreases. By increasing the critical angle, the optical reflectivity decreases. When rarefaction wave is incident on the interface, the optical reflectivity increases. The reflected intensity is recorded by reverse biased photodiode, which produces negative output voltage. Therefore, the compressive and rarefaction waves are measured as positive and negative pulses, respectively.

A flexible PVDF polymer sheet was used, which, unlike its piezoelectric ceramic and quartz counterparts, has an acoustic impedance much closer to that of water. Aluminum film electrodes are coated onto each surface of the PVDF sheet, which are overlapped to form an active area. When an acoustic wave is incident on the active area of the transducer, a voltage $U(d)$ is induced, given by

$$U(d) = \frac{\varepsilon_{33} A}{C} \bar{p}(d), \tag{5}$$

where d is the film thickness, ε_{33} is the piezoelectric constant of the PVDF film, A is the active area, $p(d)$ is the stress inside the film, averaged over its thickness, and C is the sum of capacitances of transducer, cable, and oscilloscope.

The sensitivity of PVDF was evaluated for a membrane with a thickness of 5 μm and an active area of 25 mm^2. The electrodes of transducer were connected to a 1-MΩ input of a digitizer (500 MHz, LeCroy 9354 AL, Geneva, Switzerland) by the direct current (DC) coupler of the active differential amplifier (AP033, LeCroy).

A calibrated PVDF needle hydrophone (model 80-0.5-4.0, Imotec Messtechnik, Warendorf, Germany), with 0.5-mm-diameter sensitive element and 25-MHz bandwidth, was used as a reference hydrophone which gave an output of 0.011 μV/Pa. The needle hydrophone was directly connected with a 30-cm-long cable to the 1-MΩ input of the digitizer.

We developed a 2D ultrasound-imaging scanner to obtain reproducible experimental conditions. Figure 3 shows the lateral view of the plexiglass scanner. The scanner consisted of a holder, which held the optical fiber tip, absorber and active area of detector at fixed distances. The distances from the absorber and the active area of the detector to the fiber tip were 1 and 1.5 cm, respectively.

Laser pulses (energy 2 mJ, pulse duration 6 ns) were emitted by an optical parametric oscillator (OPO), which had a tuning range from 400 to 2500 nm. The OPO pulses were directed via an optical fiber onto a closed cylindrical container (with height of 15 mm and diameter of 4 mm) filled with nonscattering aqueous solution of indocyanine green (ICG). The top and bottom of the container were covered with mylar foils (4 μm, Dupont, Texas, USA).

The optical absorption peak of 5-μmol/L ICG ($\mu_{\rm a}$ = 43 mm^{-1}) was at 675 nm, to which the OPO was tuned. At 1.5 cm far from the fiber tip, the transversal beam profile of the OPO pulses was a top hat plateau of 1.75 mm in diameter with Gaussian wings of 1 mm width.

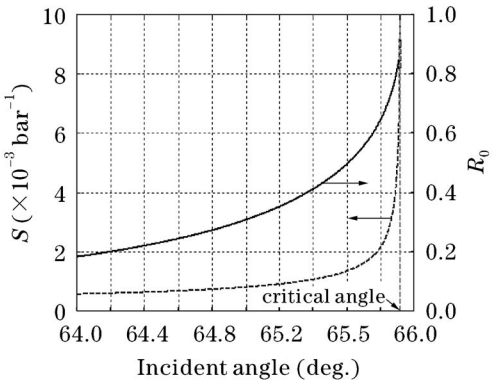

Fig. 2. Sensitivity S and the reflectance R_0 at ambient pressure of the optical transducer at incident angles near the critical value of total internal reflection.

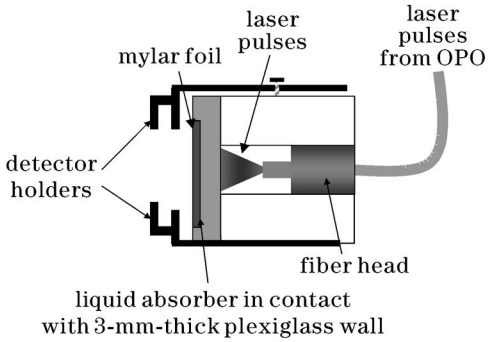

Fig. 3. Lateral view of the experimental sensor head.

Finally, the output of each set was averaged over 64 and 1024 shots by means of the signal-averaging function of a 500-MHz digitizing oscilloscope. The data was captured from the oscilloscope to a computer, where the SNR and NEP were calculated by using MATLAB software (version 6.5).

The sensitivity of detection systems is determined by the ability to detect minute fluctuations in the output of the systems. Depending on the type of detector used, various types of noise are described[11]. Noise sources in the optical detection systems include $1/f$ noise, generation-recombination noise, thermal noise, and shot noise. In the light source itself, amplitude and wavelength instabilities contribute to measurement uncertainty. These categories of noise, especially thermal noise, are associated with the electronics used to amplify and process the detector signal. In general, the absolute nature of these various categories of electronic noise is not known. Instead, their effects are described statistically so that the total noise power contribution from each source can be estimated. In fact, it is only when the power associated with the desired signal exceeds the total power of all of the noise sources that one can be assured of the detectability of a signal. Thus SNR is introduced to help define detecting ability limits of detection systems. For the purposes of this paper, the SNR is defined as the ratio of signal power (area under surface of the signal power spectrum) to noise power.

Figure 4 shows the photoacoustic signals at about 7 μs after the generation of the ultrasound for each detection system under the same experimental conditions. The signal amplitudes were arbitrarily normalized to emphasize on the importance of the noise level in calculating of the system sensitivity. Table 1 shows the SNRs and NEPs of

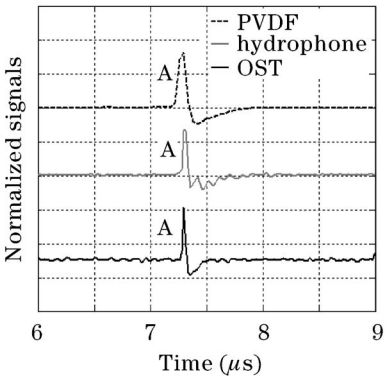

Fig. 4. Photoacoustic signals averaged over 1024 shots for each detection system. The symbol A represents the bipolar signal.

Table 1. SNRs and NEPs of the Three Detection Systems, with Ttotal Noise Level of 64 and 1024 Averages with Laser Shot Source, 10 Repeated Experiments

System	SNR (dB)		NEP (kPa)
	64	1024	
PVDF	63	75	4
Hydrophone	44	56	11
OST	42	53	12

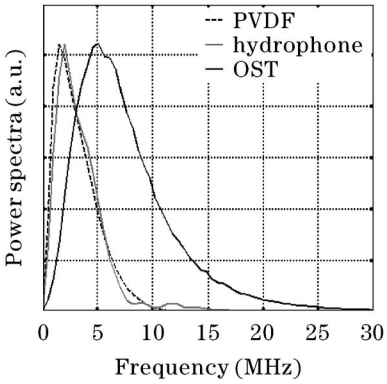

Fig. 5. Power spectra of detection systems under our experimental geometry.

the detection systems.

Several authors[12] have examined the theoretical sensitivity of detectors to show that

$$\mathrm{SNR} \propto \left(\frac{1}{B}\right)^{1/2}, \tag{6}$$

where B is the frequency detection bandwidth. As expected, larger detection bandwidths in an ultrasound system produce greater noise levels and inferior SNRs. In this experiment the detection bandwidth was measured at the level of full-width at half-maximum (FWHM) of the signal power spectrum. Figure 5 shows that the experimental bandwidth of the optical detection system is about two times higher than that of the piezoelectric detection system.

Measurements showed that the SNR with 1024 averaging of the needle hydrophone is at least 3 dB better than the OST in performance. The same measurements with the PVDF transducer showed that its SNR is 19 dB more than the hydrophone. Under our experimental conditions, the equivalent noise levels of the PVDF, the hydrophone, and the OST were 4, 11, and 12 kPa, respectively. Hence, in terms of the SNR, the optical system output was 22 dB less than that of the PVDF transducer.

The detection systems with a high sensitivity can be used for detecting small tumors, located deeply in human tissues, such as the breast. The sensitivity of various detection systems has been reported by different research methods. For this reason, we developed a comparative study with reproducible experimental conditions. A complete comparison included the measurements of the SNRs and NEPs of the PVDF, hydrophone, and OST systems, and the latter normally consisted of transducer photodiode/amplifier combination.

The results listed in Table 1 showed that the SNRs of hydrophone and OST were 56 and 53, respectively, but the SNR of PVDF detector was 75 dB. The NEP of the PVDF sheet was 4 kPa, lower than that of the OST over a 50 MHz bandwidth. The NEP of OST was increased by the shot noise in the detection process. The shot noise depends on the signal amplitude and increases by increasing light intensity and corresponding signal current. This can be seen from the expression for shot noise

power given as

$$i_{\text{shot}}^2 = 2q\bar{I}B, \tag{7}$$

where q is the electric charge, B is the frequency bandwidth of the detection system, and $\bar{I}$ is the average current in the signal path. The shot noise power increases linearly with the average current in the system and the bandwidth. Beard *et al.* developed a new optical detection system, which provided a NEP of 0.35 kPa over a 20-MHz measurement bandwidth[5]. The NEP is lower than our NEP due to the bandwidth reduction, meanwhile the high frequency information will be lost. The NEP of an optical detection system is reduced by employing electronic noise rejection schemes.

In this study, the PVDF transducer had the highest SNR and the lowest NEP. For piezoelectric materials, minimally detectable pressure $p_{\min}$ corresponding to the thermal noise voltage is given by

$$p_{\min} = \frac{4.6 f_{\text{upper}}}{g_{33} c_1} \sqrt{\frac{kT_0}{C_T}}, \tag{8}$$

where f_{upper} is the upper limit ultrasound frequency, g_{33} is the piezoelectric voltage constant, which is 0.18 Vm/N for PVDF, c_1 is the velocity of sound in a piezoelectric material that is 1400 m/s for PVDF, k is the Boltzman constant, T_0 is the temperature of the piezoelement, and C_T is piezoelement capacitance. $p_{\min}$ of PVDF is 8 times higher than that of the lithium niobate.

On the other hand, the detection sensitivity is increased by reducing acoustic impedance difference of biological tissues and piezoelectric materials. In contrast to lithium niobate and quartz, acoustic impedance of PVDF is close to that of biological tissues. Therefore the PVDF is a material of choice for a number of applications in biomedicine.

For imaging of superficial tissues such as the skin microvessels, it is desirable to detect ultrasonic signals at the same position where the tissue is irradiated, this is called backward mode. A specially designed PVDF has been developed, which is transparent for optical irradiation[13]. Thus, the detector provides a means of implementing the backward mode of operation.

In conclusion, the PVDF transducer is the most attractive detector, which provides reasonable detection sensitivity and bandwidth for photoacoustic biomedical applications. Future work is focused on designing an array of PVDF with an optimal lateral resolution and without electronic complexibility for biomedical imaging.

M. Hejazi is the author to whom the correspondence should be addressed, her e-mail address is mhejazi@sina.tums.ac.ir.

References

1. A. A. Karabutov, E. V. Savateeva, and A. A. Oraevsky, Proc. SPIE **3601,** 284 (1999).
2. A. A. Oraevsky, V. A. Andreev, A. A. Karabutov, R. D. Fleming, Z. Gatalica, H. Singh, and R. O. Esenaliev, Proc. SPIE **3597,** 352 (1999).
3. G. Ku, X. Wang, G. Stoica, and L. V. Wang, Phys. Med. Biol. **49,** 1329 (2004).
4. P. C. Beard, A. M. Hurrell, and T. N. Mills, IEEE Trans. Ultrasonics, Ferroelectrics, and Frequency Control **47,** 256 (2000).
5. E. Z. Zhang and P. C. Beard, Proc. SPIE **5320,** 222 (2004).
6. A. A. Oraevsky and A. A. Karabutov, Proc. Int. Soc. Opt. Eng **3916,** 228 (2000).
7. K. P. Köstli, M. Frenz, and H. P. Weber, J. Appl. Phys. **88,** 1632 (2000).
8. J. D. Hamilton and M. O'Donnell, IEEE Trans. Ultrasonic, Ferroelectrics, and Frequency Control **45,** 216 (1998).
9. G. Paltauf, H. Schmidt-Kloiber, K. P. Köstli, and M. Frenz, Proc. SPIE **3601,** 248 (1999).
10. G. Paltauf, H. Schmidt-Kloiber, K. P. Köstli, M. Frenz, and H. P. Weber, Appl. Phys. Lett. **75,** 1048 (1999).
11. E. L. Deneriak and D. G. Crowe, *Optical Radiation Detectors* (Wiley, New York, 1984) p.36.
12. A. S. Murfin and R. A. J. Soden, Meas. Sci. Technol. **11,** 1208(2000).
13. M. Jaeger, J. J. Niederhauser, M. Hejazi, and M. Frenz, Biomed. Opt. **10,** 2005 (in press).